International Journal of Engineering Inventions
e-ISSN: 2278-7461, p-ISSN: 2319-6491
Volume 14, Issue 12 [December 2025] PP: 141-156

Mathematical Modelling and Transmission Dynamics of Rabies with the Influence of Vaccination in Human, Dog and Raccoon Populations.

Yahaya Aliyu Abdullahi[1*], Abdulmumini Husseini[2] Umar Muhammad[1], Musa Abdullahi[1]. Mubarak M. Tela, [3]Usman M. Damina, [4]Radiya S. M

[1]*Department of Statistics, Gombe State Polytechnic Bajoga, P.M.B 0190 Gombe, Gombe State.*
[2]*Department of Mathematics, Nigeria Army University, Biu, Nigeria*
[3]*Department of Computer Science, Gombe State College of Education and Legal Studies, Nafada*
[4]*Department of Statistics, Federal Polytechnic Kaltungo, Gombe State, Nigeria*

Abstract
Rabies is a highly fatal zoonotic viral disease primarily transmitted through bites or saliva of infected animals, with dogs serving as the main reservoir responsible for the majority of human cases worldwide. In this study, a deterministic mathematical model is developed to investigate the effects of vaccination on the transmission dynamics of rabies in human, dog, and raccoon populations. The model is shown to be mathematically and epidemiologically well-posed. Using the next-generation matrix approach, the basic reproduction number, R_D, is derived as a key threshold parameter, and both the rabies-free and endemic equilibrium points are determined. Analytical results establish conditions under which the equilibria are locally and globally asymptotically stable. Numerical simulations illustrate the impact of vaccination coverage and demographic factors, such as annual dog and raccoon births, on reducing infection prevalence and controlling rabies spread.
Keywords: *Rabies, raccoon, equilibrium points, reproduction number, stability.*

Date of Submission: 15-12-2025 Date of acceptance: 31-12-2025

I. Introduction

The virus that causes rabies is called a Lyssavirus. It causes inflammation in the mammalian brain. Fever and tickling at the exposure site are the first signs of infection. One or more other symptoms, such as erratic movement, loss of control over body parts, confusion, fear of water, and excessive excitement, may emerge later. After being exposed to the disease, symptoms usually don't show up for one to three months. From less than a week to over a year, the symptoms can change. As soon as the symptoms appeared, almost all of the cases ended in death. It spreads when an infected person or animal scratches or bites another person or animal. If an infected animal's saliva gets into the mouth, eyes, or nose of a vulnerable animal, it can also spread rabies. Dogs are often the most prevalent animal involved in the spread of rabies. Dog bites are the direct cause of almost 99% of rabies cases in nations where the illness is prevalent in dogs (Addo, 2012).

In several regions of the world, vaccination and animal management have decreased the risk of dog rabies. Individuals at high risk, such as those who work with dogs or spend a lot of time in places where rabies is prevalent, can get vaccinated before being exposed. Rabies and vaccination (rabies vaccinations). If a person receives treatment before symptoms develop, immunoglobulins can effectively prevent the condition. The spread of the infections may be somewhat inhibited by washing the exposed site for 15 minutes with soap and water, iodine, povidone, or detergent.

In early models of rabies dynamics, the populations were separated into particular classifications as susceptible (S), exposed (E), infectious (I), and removed (R) individuals (Anderson *et al.,,* 1991). The dynamics of rabies, representing either single populations or connected meta-populations, were explained by a system of ordinary differential equations (ODEs), from which some inferences about temporal and spatial patterns could be made. In the early model of rabies, the basic SEIR compartmental framework was used to deduce several crucial aspects of disease genesis and propagation. The model equation was used to determine the virus's basic reproductive number (R_0) and the crucial threshold for epidemic onset. When $R_0 > 1$, the virus will spread and the illness will continue. One might use this to estimate the amount of population culling required to lower the threshold density below the epizootic level. Since there is evidence of the development of natural immunity and

vaccination, which translate susceptible into the removed class, they did not explore the R class, despite the fact that their model was formulated using the SEIR compartmental framework.

A stochastic geographic model was developed by Smith *et al.,* (2002) to explain the rabies outbreak in connecticut. forecasting rabies epidemics' spatial dynamics in diverse environments. Based on their findings, they proposed that rivers serve as a semipermeable barrier that reduces the rate of rabies transmission by a factor of seven. The impact of long-distance translocation and regional heterogeneity on the raccoon rabies outbreak in Connecticut was assessed using data from the state, habitat effects, and long-distance translocation events. The results of the re-analysis demonstrated that rivers interact to further restrict the spatial spread of raccoon rabies.

Data from Ohio was analyzed by Russell *et al.,* (2005) using the stochastic spatial model developed by Smith *et al.,* (2002). Later, they wrote a second work that used an ODE model to demonstrate how rabies transmission could be stopped by delivering vaccines behind obstacles like rivers. The three classes were divided into nine spatial compartments in this SIR model, resulting in a total of 27 ODEs. Their findings shown that a large population requires a greater vaccination rate, while a smaller population requires a lower vaccination rate at a higher cost.

Asano *et al.,* (2008) used a SIR Meta-population model to apply optimum control to an epidemic model for rabies in raccoons. Through the arrangement of sub-populations linked by mobility, they included space. In addition to accounting for the cost of vaccine administration, the optimal control vector provides the vaccination rate in each sub population that lowers the total sub-populations of infected classes.

Zhang *et al.,* (2011) examined the real-world scenario of rabies outbreaks in China. In order to investigate the dynamics of rabies transmission in humans and dogs as well as control measures, they developed two mathematical models. They determined that vaccination is the most effective method of rabies control after comparing the effectiveness of three different approaches: culling, vaccination, and culling and vaccination.

In China, Hong-tao *et al.,* (2014) developed a different mathematical model of rabies using comparable control techniques. Infected dogs, individuals infected by exposed dogs, and apparently healthy canines carrying the virus were all taken into account in their model. Their modeling and analytical analysis demonstrated that the culling method was the most effective, followed by vaccination and culling and vaccination.

Zhang *et al.,* (2011) state that one of China's primary public health issues is human rabies. They built a model to investigate efficient preventative and control strategies. They put out a deterministic model to investigate the dynamics of rabies transmission in China. In addition to taking into account the spread of rabies from infectious dogs to humans, their model used SEIR sub-populations of both humans and dogs. The model simulations concur with the Chinese Ministry of Health's reported human rabies data. Based on their data, they calculated that the $R_0 = 2$ for rabies transmission in China and predicted that, although the number of human rabies cases is declining, it would rise again around 2030. Additionally, they conducted additional sensitivity analysis about the model parameters and contrasted the outcomes of dog vaccination and culling.

In a recent study, Isiyaku et al. (2025) developed a deterministic model to study rabies transmission between humans and dogs, analyzing disease-free and endemic equilibria using the basic reproduction number (RD). Their results show that vaccinating dogs is the most effective strategy to reduce rabies spread, with dog-to-dog transmission and dog recruitment rates being the most influential factors. The study highlights the importance of targeting interventions in the dog population to control rabies, Musa et al. (2024) used a delay differential equations model to study rabies transmission between humans and dogs, showing that the disease-free equilibrium is stable when the control reproduction number is below one. Their simulations indicate that vaccinating both humans and dogs, improving treatment, and controlling dog births are the most effective strategies for reducing rabies spread, with longer incubation periods further limiting endemicity. The study highlights the importance of combined interventions targeting both species to control rabies effectively.

In their work Modeling the Dynamics of Rabies Transmission with Vaccination and Stability Analysis, Ega *et al.,* (2015) developed a deterministic mathematical model for the dynamics of rabies transmission in humans and animals in and around Addis Ababa, Ethiopia. Their model took into account a dog population immunization program. They calculated the basic reproduction number and the effective reproduction number. Their findings are entirely dependent on the dog population's parameters, demonstrating that the dog population is the source of infections in humans and animals. They calculated that the disease will be endemic for several sets of parameter values based on data from the Ethiopian Public Health Institute in Addis Ababa. They discovered that the basic reproduction number was 2 and the effective reproduction number was 1.6. Their computer modeling of the reproduction ratio demonstrates that the most effective way to stop the spread of rabies in and around Addis Ababa is to combine vaccination, stray dog culling, and annual puppy crop control.

The major way that rabies is spread to people is through dog bites or scratches, particularly from infected dogs (Jibat *et al.,* 2017). Additionally, direct contact with a wound or mucosal surface (such as the mouth, nose, or eye) contaminated by a rabid dog's saliva can spread rabies (Chapwanya *et al.,* 2016). Rabies can infect humans and other creatures by aerosol transmission or tissue and organ transplantation (Alan and Jackson, 2008; Tenzin, 2012). Early rabies symptoms include fever with pain, unusual or unexplained tingling, hyper-salivation, sore

throat, cough, nausea and vomiting, and a burning or pricking sensation (paranesthesia) at the site of an animal bite. These symptoms are similar to those of the flu in the early stages of infection (Stanley, 2000; WHO, 2019). Subsequently, the virus progressed to the central nervous system, causing increasing and lethal inflammation of the brain and spinal cord, which then led to paralysis and hyperactivity (Stanley, 2000).

The majority of rabies cases are caused by an infected dog's bite. The severity of the lesion, the site of the bite, the amount and type (genotype) of virus implanted into the wound or wounds, and the promptness of post-exposure prophylaxis (PEP) all influence the outcome of RABV exposure. In the absence of PEP, the average risk of contracting rabies after being bitten by a rabid animal is 55% for the head, 22% for the upper extremities, 9% for the trunk, and 12% for the lower limb. 9. Human bite victims' risk of infection is influenced by the fluctuating virus load in the saliva of dogs infected with RABV. Infection with RABV in rodents is extremely rare. There have been no documented human rabies cases caused by rodent bites (WHO, 2018). Considering all the above-reviewed articles, none of the above considered raccoon's population. This work formulated a deterministic model to study rabies dynamics, which took into consideration raccoons population. We specifically targeted to study the impact of vaccination on the proposed model.

II. Model Formulation

The model consists of three populations: humans, dogs and Raccoons living in the same environment. At any time t, the human population is divided into three sub-populations of vaccinated humans $V_H(t)$, susceptible humans $S_H(t)$, infected humans $I_H(t)$, . Hence, the total population of humans denoted by $N_H(t)$ is given by

$$N_H(t) = V_H(t) + S_H(t) + I_H(t)$$

Similarly, at any time t, the dog population is subdivided into three sub-populations of vaccinated dogs $V_D(t)$, susceptible dogs $S_D(t)$, and infected dogs $I_D(t)$, so, the total population of dogs is denoted by $N_D(t)$, is given by

$$N_D(t) = V_D(t) + S_D(t) + I_D(t)$$

Furthermore, at any time t, the dog population is subdivided into three sub-populations of vaccinated Raccoons $V_R(t)$, susceptible Raccoons $S_R(t)$, and infected Raccoons $I_R(t)$ so, the total population of dogs is denoted by $N_R(t)$, is given by

$$N_R(t) = V_R(t) + S_R(t) + I_R(t)$$

Recruitment into the human population is done by administering vaccination for the newly born babies at a rate $r\Pi_H$ and decrease due to non-effectiveness (failure) of vaccination in Human at a rate α_H and natural death rate μ_H for all human class. The population of susceptible population is increase by the proportion of non-effectiveness (failure) of vaccination in human at a rate α_H and $(1-r)\Pi_H$ and decreased by sufficient contact between susceptible human and infected dogs at a rate $\beta_{DH} S_H I_D$ where β_{DH} is the transmission rate of RABV from dog to Human. The infected population $I_H(t)$ is increased by sufficient contact between susceptible human and infected dogs at a rate and decreases by natural death and death due to RABV i.e., μ_H and d_H respectively.

Similarly, recruitment in to dogs population is done also by administering vaccination due to increase in dogs annual birth of puppies at a rate $p\Pi_D$ and decrease due to non-effectiveness (failure) of vaccination in dogs population at a rate σ_D and death rate μ_D, the population of the susceptible dogs is increased by the proportion of non-effectiveness (failure) of vaccination in dogs at a rate σ_D and $(1-p)\Pi_D$ and decreased by sufficient contact between susceptible dogs and infected Raccoons at a rate of $\beta_{RD} S_D I_R$ where β_{RD} is the transmission rate of RABV from Raccoons to dogs . The infected dogs population $I_D(t)$ is increased by sufficient contact between susceptible dogs and infected Raccoons at a rate of $\beta_{RD} S_D I_R$ and decreased by natural death and deaths due to RABV at a rate μ_D and c_D respectively.

Furthermore, recruitment in to Raccoons population is done by vaccinating the newly born raccoons at a rate $p\Pi_D$ and decrease due to non-effectiveness (failure) of vaccine in Raccoons population at a rate ϕ_R and death

rate μ_R, the population of the susceptible Raccoons is increased by the proportion of non-effectiveness (failure) of vaccination in Raccoons at a rate ϕ_R and $(1-z)\Pi_R$ and decreased by sufficient contact between susceptible humans and infected Raccoons at a rate of $\beta_{RH} S_H I_R$ where β_{RH} is the transmission rate of RABV from Raccoons to Humans. The infected Raccoons population $I_R(t)$ is increased by sufficient contact between susceptible humans and infected Raccoons at a rate of $\beta_{RH} S_H I_R$ and decreased by natural death and deaths due to RABV at a rate μ_R and e_R respectively.

The biological assumptions of the model are as follows:

i. The dogs mix homogenously.

ii. All infected dogs and Raccoons dies because showing symptoms of sickness are clubbed to death, and their meat are used as meal.

iii. Age, sex and type of the dog, coupled with the climatic conditions, do not affect the probability of a dog being infected.

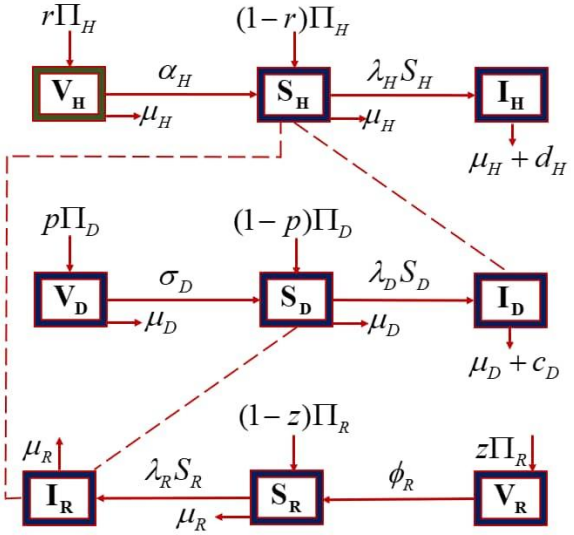

Figure 1: Schematic diagram of the model

The proposed model's dynamics are given as a system of non-linear ordinary differential equations, which are as follows:

$$\left.\begin{aligned}
\frac{dS_H}{dt} &= \alpha_H V_H + (1-r)\Pi_H - (\lambda_H + \mu_H) S_H \\
\frac{dV_H}{dt} &= r\Pi_H - (\mu_H + \alpha_H) V_H \\
\frac{dI_H}{dt} &= \lambda_H S_H - (\mu_H + d_H) I_H \\
\frac{dS_D}{dt} &= \sigma_D V_D + (1-p)\Pi_D - (\lambda_D + \mu_D) S_D \\
\frac{dV_H}{dt} &= p\Pi_D - (\mu_D + \sigma_D) V_D \\
\frac{dI_D}{dt} &= \lambda_D S_D - (\mu_D + c_D) I_D \\
\frac{dS_R}{dt} &= \phi_R V_R + (1-z)\Pi_R - (\lambda_R + \mu_R) S_R \\
\frac{dV_R}{dt} &= z\Pi_R - (\phi_R + \mu_R) V_R \\
\frac{dI_R}{dt} &= \lambda_R S_R - (\mu_R + e_R) I_R
\end{aligned}\right\} \quad \text{.....(2.1)}$$

where:

$$\lambda_H = \frac{\beta_{DH} S_H I_D + \beta_{RH} S_H I_R}{N_H}, \quad \lambda_D = \frac{\beta_{RD} S_D I_R + \beta_{DD} S_D I_D}{N_D}, \quad \lambda_R = \frac{\beta_{RR} S_R I_R}{N_R}$$

with :

$S_H(0) > 0, V_H(0) \geq 0, I_H(0) \geq 0, S_D(0) > 0, V_D(0) \geq 0, I_D(0) \geq 0, S_R(0) > 0, V_R(0) \geq 0, I_R(0) \geq 0$.

The basic model (2.1) will now be analysed to gain insights into its dynamical features.

Basic Properties

For the basic model (2.1) to be biologically meaningful, it is important to prove that all its state variables are non-negative for all time. In other words, solutions of the model system (2.1) with positive initial data will remain positive for all time $t > 0$. This is shown below.

Theorem 2.1. *Let the initial data* $S_H(0) > 0, V_H(0) \geq 0, I_H(0) \geq 0, S_D(0) > 0, V_D(0) \geq 0, I_D(0) \geq 0,$ $S_R(0) > 0, V_R(0) \geq 0, I_R(0) \geq 0$. *Then the solutions* $\left(S_H, V_H, I_H, S_D, V_D, I_D, S_R, V_R, I_R\right)$ *of the basic model (2.1), with positive initial data, will remain positive for all time* $t > 0$.

Proof. Let

$$t_1 = \sup\{t > 0 : S_H(t) > 0, V_H(t) > 0, I_H(t) > 0, S_D(t) > 0, V_D(t) > 0, I_D(t) > 0, S_R(t) > 0, V_R(t) > 0, I_R(t) > 0\}$$

Thus, $t_1 > 0$. The first equation of model (2.1) we have;

$$\alpha_H V_H + (1-r)\Pi_H - (\lambda_H + \mu_H) S_H \geq (1-r)\Pi_H - (\lambda_H + \mu_H) S_H \tag{2.1}$$

Equation (2.1) can be re-written as

$$\frac{d}{dt}\left[S_H(t) \exp\left(\int_0^t \lambda_H(\tau) d\tau + \mu_H t \right) \right] \geq (1-r)\Pi_H \exp\left(\int_0^t \lambda_H(\tau) d\tau + \mu_H t \right)$$

Now, integrating both sides of from $t = 0$ to $t = t_1$, we have,

$$S_H(t_1) \exp\left(\int_0^{t_1} \lambda_H(\tau) d\tau + \mu_H t_1 \right) - S_H(0) \geq \int_0^{t_1} (1-r)\Pi_H \exp\left(\int_0^x \lambda_H(\tau) d\tau + \mu_H x \right) dx$$

Hence,

$$S_H(t_1) \geq \exp\left(-\int_0^{t_1} \lambda_H(\tau) d\tau - \mu_H t_1 \right) \times \left[S_H(0) + \int_0^{t_1} (1-r)\Pi_H \exp\left(\int_0^x \lambda_H(\tau) d\tau + \mu_H x \right) dx \right] > 0$$

This implies that $S_H(t_1) > 0$ for all $t_1 > 0$. Hence, $S_H(t) > 0$ for $t > 0$.

From the fourth equation of model (2.1) we have;

$$\sigma_D V_D + (1-p)\Pi_D - (\lambda_D + \mu_D) S_D \geq (1-p)\Pi_D - (\lambda_D + \mu_D) S_D \tag{2.2}$$

Equation (2.2) can be re-written as

$$\frac{d}{dt}\left[S_D(t) \exp\left(\int_0^t \lambda_D(\tau) d\tau + \mu_D t \right) \right] \geq (1-p)\Pi_D \exp\left(\int_0^t \lambda_D(\tau) d\tau + \mu_D t \right)$$

Now, integrating both sides of from $t = 0$ to $t = t_1$, we have,

$$S_D(t_1) \exp\left(\int_0^{t_1} \lambda_D(\tau) d\tau + \mu_D t_1 \right) - S_D(0) \geq \int_0^{t_1} (1-p)\Pi_D \exp\left(\int_0^x \lambda_D(\tau) d\tau + \mu_D x \right) dx$$

Hence,

$$S_D(t_1) \geq \exp\left(-\int_0^{t_1} \lambda_D(\tau)d\tau - \mu_D t_1\right) \times$$

$$\left[S_D(0) + \int_0^{t_1} (1-p)\Pi_D \exp\left(\int_0^x \lambda_D(\tau)d\tau + \mu_D x\right)dx\right] > 0$$

This implies that $S_D(t_1) > 0$ for all $t_1 > 0$. Hence, $S_D(t) > 0$ for $t > 0$.

From the seventh equation of model (2.1) we have;

$$\phi_R V_R + (1-z)\Pi_R - (\lambda_R + \mu_R)S_R \geq (1-z)\Pi_R - (\lambda_R + \mu_R)S_R \tag{2.3}$$

Equation (2.3) can be re-written as

$$\frac{d}{dt}\left[S_R(t)\exp\left(\int_0^t \lambda_R(\tau)d\tau + \mu_R t\right)\right] \geq (1-z)\Pi_R \exp\left(\int_0^t \lambda_R(\tau)d\tau + \mu_R t\right)$$

Now, integrating both sides of from $t = 0$ to $t = t_1$, we have,

$$S_R(t_1)\exp\left(\int_0^{t_1} \lambda_R(\tau)d\tau + \mu_R t_1\right) - S_R(0)$$

$$\geq \int_0^{t_1} (1-z)\Pi_R \exp\left(\int_0^x \lambda_R(\tau)d\tau + \mu_R x\right)dx$$

Hence,

$$S_R(t_1) \geq \exp\left(-\int_0^{t_1} \lambda_R(\tau)d\tau - \mu_R t_1\right) \times$$

$$\left[S_R(0) + \int_0^{t_1} (1-z)\Pi_R \exp\left(\int_0^x \lambda_R(\tau)d\tau + \mu_R x\right)dx\right] > 0$$

This implies that $S_R(t_1) > 0$ for all $t_1 > 0$. Hence, $S_R(t) > 0$ for $t > 0$. Similarly, it can be shown that $V_H > 0, I_H > 0, V_D > 0, I_D > 0, V_R > 0, I_R > 0$ for all time $t > 0$. Hence, all solutions remains positive for all non-negative initial conditions, as required.

Since all parameters and state variables of the model (2.1) are non-negative for all $t \geq 0$, adding the human sub-populations, we have

$$\frac{dN_H}{dt} \leq \Pi_H - \mu_H N_H$$

it follows, using comparison theorem [44], that

$$N_H(t) \leq N_H(0)e^{-\mu_H t} + \frac{\Pi_H}{\mu_H}\left(1 - e^{-\mu_H t}\right),$$

so that, $N_H(t) \leq \frac{\Pi_H}{\mu_H}$ if $N_H(0) \leq \frac{\Pi_H}{\mu_H}$. Similarly, adding the dog and raccoon sub-populations, we have;

$$\frac{dN_D}{dt} \leq \Pi_D - \mu_D N_D$$

and

$$\frac{dN_R}{dt} \leq \Pi_R - \mu_R N_R$$

it follows, using comparison theorem, that

$$N_D(t) \leq N_D(0)e^{-\mu_D t} + \frac{\Pi_D}{\mu_D}\left(1 - e^{-\mu_D t}\right)$$

and

$$N_R(t) \leq N_R(0)e^{-\mu_R t} + \frac{\Pi_R}{\mu_R}\left(1 - e^{-\mu_R t}\right)$$

so that, $N_D(t) \le \frac{\Pi_D}{\mu_D}, N_R(t) \le \frac{\Pi_R}{\mu_R}$ if $N_D(0) \le \frac{\Pi_D}{\mu_D}$ and $N_R(0) \le \frac{\Pi_R}{\mu_R}$ respectively. Consequently, the following biologically-feasible region:

$$\Omega = \Omega_H \cup \Omega_D \cup \Omega_R \subset \mathbb{R}^3_+ \times \mathbb{R}^3_+ \times \mathbb{R}^3_+$$

Where:

$$\Omega_H = \left\{ \left(S_H, V_H, I_H\right) \in \mathbb{R}^3_+ : N_H \le \frac{\Pi_H}{\mu_H} \right\}, \qquad \Omega_H = \left\{ \left(S_D, V_D, I_D\right) \in \mathbb{R}^3_+ : N_D \le \frac{\Pi_D}{\mu_D} \right\},$$

$$\Omega_R = \left\{ \left(S_R, V_R, I_R\right) \in \mathbb{R}^3_+ : N_R \le \frac{\Pi_R}{\mu_R} \right\}$$

Is positively invariant for the model (2.1) (that is, all solutions of the model with initial conditions in Ω will remain in Ω for all time $t \ge 0$). It is, therefore, sufficient to consider the solutions of the model in Ω. This result is summarized below.

Lemma 2.1: *The region* Ω is positively invariant for the basic model (2.1) with initial conditions in $\mathbb{R}^6_+$.

3.3 Existence and Stability of Equilibria

3.2.1 Rabies-free equilibrium point (RFE)

The rabies model (2.1) has RFE $\left(I_H = I_D = I_R = 0\right)$, obtained by setting the right-hand sides of the reduced model equations to zero, given by

$$\left.\begin{aligned} 0 &= \alpha_H V_H + (1-r)\Pi_H - (\lambda_H + \mu_H) S_H \\ 0 &= r\Pi_H - (\mu_H + \alpha_H) V_H \\ 0 &= \sigma_D V_D + (1-p)\Pi_D - (\lambda_D + \mu_D) S_D \\ 0 &= p\Pi_D - (\mu_D + \sigma_D) V_D \\ 0 &= \phi_R V_R + (1-z)\Pi_R - (\lambda_R + \mu_R) S_R \\ 0 &= z\Pi_R - (\phi_R + \mu_R) V_R \end{aligned}\right\} \qquad (4)$$

Solving equation (4) for the RFE, we obtained

$$E_{RF} = \left[S_H^0, V_H^0, 0, S_D^0, V_D^0, 0, S_R^0, V_R^0, 0 \right]$$

where:

$$S_H^0 = \frac{\mu_H (1-r)\Pi_H + \alpha_H \Pi_H}{\mu_H (\mu_H + \alpha_H)}, \quad V_H^0 = \frac{r\Pi_H}{\alpha_H + \mu_H}$$

$$S_D^0 = \frac{\mu_D (1-p)\Pi_D + \sigma_D \Pi_D}{\mu_D (\mu_D + \sigma_D)}, \quad V_H^0 = \frac{r\Pi_H}{\alpha_H + \mu_H}$$

$$S_R^0 = \frac{\mu_R (1-z)\Pi_R + \phi_R \Pi_R}{\mu_R (\mu_R + \phi_R)}, \quad V_H^0 = \frac{z\Pi_R}{\phi_R + \mu_R}$$

The linear stability of E_{SF} can be established using the next generation operator method on the system (2.1). using the notation in [83], the matrices F^0 and V^0, for the new infection terms and the remaining transfer terms, are, respectively, given by,

$$F^0 = \begin{bmatrix} 0 & \frac{\beta_{DH} S_H^0}{N_H} & \frac{\beta_{RH} S_H^0}{N_H} \\ 0 & \frac{\beta_{DD} S_D^0}{N_D} & \frac{\beta_{RD} S_D^0}{N_D} \\ 0 & 0 & \frac{\beta_{RR} S_R^0}{N_R} \end{bmatrix}$$

and,

$$V^0 = \begin{bmatrix} \mu_H + d_H & 0 & 0 \\ 0 & \mu_D + c_D & 0 \\ 0 & 0 & \mu_R + e_R \end{bmatrix}$$

so that,

$$R_0 = \rho\left(F_0 V_0^{-1}\right) = \max\left[R_D, R_R\right]$$

where:

$$R_D = \frac{\beta_{DD}\left(\sigma_D \Pi_D + (1-p)\Pi_D \mu_D\right)}{\mu_D\left(\sigma_D + \mu_D\right)\left(\mu_D + c_D\right)} \text{ and } R_R = \frac{\beta_{RR}\left(\phi_R \Pi_R + (1-z)\Pi_R \mu_R\right)}{\mu_R\left(\phi_R + \mu_R\right)\left(\mu_R + e_R\right)}$$

where ρ represents the spectral radius. Hence, using Theorem 2 of [83], the following result is established.

Lemma 3.1. The RFE of the basic model (2.1) is locally asymptotically stable (LAS) whenever $R_D < 1$, and unstable if $R_D > 1$.

The threshold quantity, R_D, is the basic reproduction number of model (2.1). it measures the average number of new RABV cases generated by a typical infected individual introduced into the susceptible population. The epidemiological implication of Lemma 3.2 is that a small influx of HIV-infected individuals will not generate a large outbreak in the population if the quantity R_D can be brought to (and maintained at) a value less than one.

3.3.2 Endemic equilibrium point

The RABV endemic equilibrium point (i.e., equilibria where the infected components of the model are nonzero). Let the rates of infection be given by

$$\lambda_H^{**} = \frac{\beta_{DH} I_H^{**}}{N_H^{**}} + \frac{\beta_{RH} I_R^{**}}{N_H^{**}}, \quad \lambda_D^{**} = \frac{\beta_{DD} I_D^{**}}{N_D^{**}} + \frac{\beta_{RD} I_R^{**}}{N_D^{**}} \text{ and } \lambda_R^{**} = \frac{\beta_{RR} I_R^{**}}{N_R^{**}}$$

The endemic equilibrium point is given by

$$E_{EE} = \left[S_H^{**}, V_H^{**}, I_H^{**}, S_D^{**}, V_D^{**}, I_D^{**}, S_R^{**}, V_R^{**}, I_R^{**}\right]$$

where:

$$S_H^{**} = \frac{\Pi_H\left[\alpha_H + (1-r)\mu_H\right]}{(\lambda_H^{**} + \mu_H)(\mu_H + \alpha_H)}, \quad V_H^{**} = \frac{r\Pi_H}{\mu_H + \alpha_H}, \quad I_H^{**} = \frac{\Pi_H \lambda_H^{**}\left[\alpha_H + (1-r)\mu_H\right]}{(\lambda_H^{**} + \mu_H)(\mu_H + \alpha_H)(\mu_H + d_H)},$$

$$S_D^{**} = \frac{\Pi_H\left[\sigma_D + (1-p)\mu_D\right]}{(\lambda_H^{**} + \mu_D)(\mu_D + \sigma_D)}, \quad V_D^{**} = \frac{p\Pi_D}{\mu_D + \sigma_D}, \quad I_D^{**} = \frac{\Pi_D \lambda_D^{**}\left[\sigma_D + (1-p)\mu_D\right]}{(\lambda_D^{**} + \mu_D)(\mu_D + \sigma_D)(\mu_D + c_D)},$$

$$S_R^{**} = \frac{\Pi_R\left[\phi_R + (1-z)\mu_R\right]}{(\lambda_R^{**} + \mu_R)(\mu_R + \phi_R)}, \quad V_R^{**} = \frac{z\Pi_R}{\mu_R + \phi_R}, \quad I_R^{**} = \frac{\Pi_R \lambda_R^{**}\left[\phi_R + (1-z)\mu_R\right]}{(\lambda_R^{**} + \mu_R)(\mu_R + \phi_R)(\mu_R + c_R)}$$

which exists whenever $R_D > 1$.

3.3.2 Global stability of Rabies-free equilibrium point (RFE)

In this section, we use the Castillo-Chavez theorem (Castillo-Chavez, Feng, & Huang, 2002) to investigate the global asymptotic stability of the disease free state. For the theorem to work, we rewrite model (2.1) in the form

$$\frac{dQ}{dt} = F(S, I)$$
$$\frac{dW}{dt} = G(Q,W), G(Q,0) = 0$$

where $Q \in ¡^{m}$ represents the number of uninfected individuals $W \in ¡^{m}$ denotes the number of infected population and $E_{RF} = (Q^{*}, 0)$ represents the disease-free equilibrium. The following assumptions must be satisfied for the disease-free equilibrium of model (2.1) to be globally asymptotically stable (See: Abdullahi *et al.,* 2024):

$H_1 = \frac{dQ}{dt} - F(Q,0), Q^{*}$ is globally asymptotically stable

$H_2 = G(Q,W) = AW - \hat{G}(Q,W)$ where $\hat{G}(Q,W) \geq 0$

For $(Q,W) \in \Omega,$ and $A = C_w G(Q^{*}, 0)$ is an M-matrix (the off-diagonal elements are non-negative).

Theorem. *The Rabies-free equilibrium point, E_{RF} of the model (2.1) is globally asymptotically stable if* $R_D < 1$ and conditions H_1 and H_2 are satisfied.

Proof. Let $Q = (S_H, V_H, S_D, V_D, S_R, V_R) \in ¡^{6}$ and $W = (I_H, I_D, I_R) \in ¡^{3}$ then

$$\frac{dQ}{dt} = F(Q,W) = \begin{bmatrix} \alpha_H V_H + (1-r)\Pi_H - (\lambda_H + \mu_H) S_H \\ r\Pi_H - (\mu_H + \alpha_H) V_H \\ \sigma_D V_D + (1-p)\Pi_D - (\lambda_D + \mu_D) S_D \\ p\Pi_D - (\mu_D + \sigma_D) V_D \\ \phi_R V_R + (1-z)\Pi_R - (\lambda_R + \mu_R) S_R \\ z\Pi_R - (\phi_R + \mu_R) V_R \end{bmatrix}$$

And

$$\frac{dW}{dt} = G(Q,W) = \begin{bmatrix} \frac{\beta_{DH} S_H I_D + \beta_{RH} S_H I_R}{N_H} - (\mu_H + d_H) I_H \\ \frac{\beta_{RD} S_D I_R + \beta_{DD} S_D I_D}{N_D} - (\mu_D + c_D) I_D \\ \frac{\beta_{RR} S_R I_R}{N_R} - (\mu_R + e_R) I_R \end{bmatrix}$$

then

$$F(Q,0) = \begin{bmatrix} \alpha_H V_H + (1-r)\Pi_H - \mu_H S_H \\ r\Pi_H - (\mu_H + \alpha_H) V_H \\ \sigma_D V_D + (1-p)\Pi_D - \mu_D S_D \\ p\Pi_D - (\mu_D + \sigma_D) V_D \\ \phi_R V_R + (1-z)\Pi_R - \mu_R S_R \\ z\Pi_R - (\phi_R + \mu_R) V_R \end{bmatrix}$$

as $t \to \infty$ the Rabies-free equilibrium, $E_{RF} \to \left[S_H^0, V_H^0, 0, S_D^0, V_D^0, 0, S_R^0, V_R^0, 0 \right]$ regardless of the initial conditions. Therefore, the first condition H_1 holds. For the second condition,

$$G(Q,W) = AW - \hat{G}(Q,W)$$

where:

$$AW = \begin{bmatrix} -(\mu_H + d_H) I_H + (\beta_{DH} I_D + \beta_{RH} I_R) S_H^0 \\ -(c_D + \mu_D) I_D + (\beta_{DD} I_D + \beta_{RD} I_R) S_D^0 \\ -(\mu_R + e_R) I_R + \beta_{RR} I_R S_R^0 \end{bmatrix}$$

So that

$$\hat{G}(Q,W) = \begin{bmatrix} (\beta_{DH} I_D + \beta_{RH} I_R) S_H^0 \left[1 - \frac{S_H}{S_H^0} \right] \\ (\beta_{DD} I_D + \beta_{RD} I_R) S_D^0 \left[1 - \frac{S_D}{S_D^0} \right] \\ \beta_{RR} I_R S_R^0 \left[1 - \frac{S_R}{S_R^0} \right] \end{bmatrix}$$

Since $0 \le S_H \le S_H^0, 0 \le S_D \le S_D^0,$ and $0 \le S_R \le S_R^0$ and since all parameters of model (2.1) are positive, it shows that $\hat{G}(Q,W) \ge 0$. This shows that E_{RF} is globally asymptotically stable.

4.1 Numerical Simulations

In this section, we perform some numerical simulations using the baseline values in Table 1. In order to confirm some of the analytical results obtained in this study. The simulations were run to investigate the effects of vaccination on vaccinated human, dog and raccoon population, impact of vaccination on infected dogs and raccoons and the impact of dog and raccoon birth rate on the dynamics of rabies virus.

Parameter	Values	Reference
Π_H, Π_D, Π_R	$0.0314, 5\times10^6, 5000$	Isiyaku *et al.,* (2025)
μ_H, μ_D, μ_R	$0.0074, 0.056, 0.076$	Isiyaku *et al.,* (2025)
r	0.7	Assumed
p	0.6	Assumed
z	0.4	Assumed
c_D	0.042	Assumed
σ_D	0.025	Assumed
ϕ_R	0.56	Assumed
α_H	0.46	Assumed
d_H	0.75	Musa *et al.,* (2024)
e_R	0.075	Musa *et al.,* (2024)
β_{DD}, β_{DH}	$1.58\times10^{-5}, 2.29\times10^{-12}$	Isiyaku *et al.,* (2025)
$\beta_{RH}, \beta_{RD}, \beta_{RR}$	$0.26\times10^{-3}, 0.58\times10^{-4}, 1.56\times10^{-5}$	Isiyaku *et al.,* (2025)

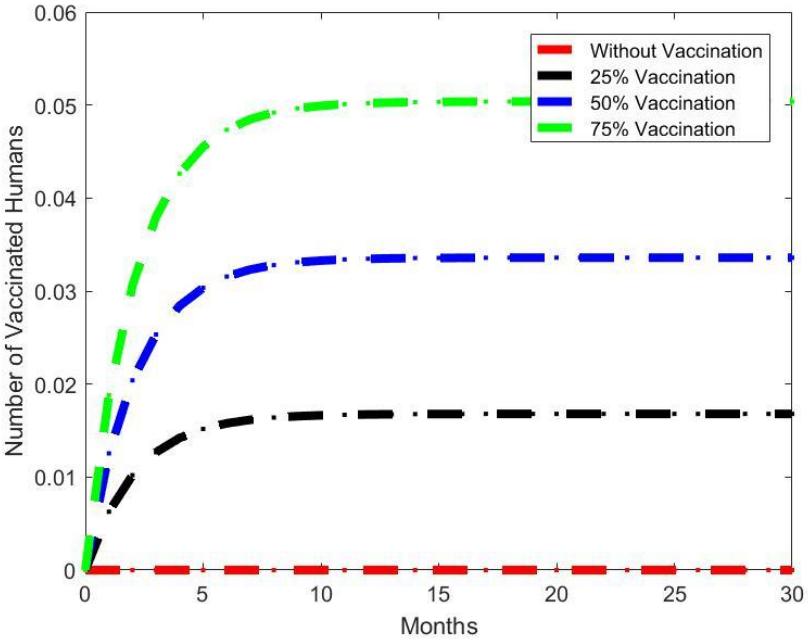

Figure 4.1: Effect of Vaccination rate on the dynamics of Vaccinated Human Population.

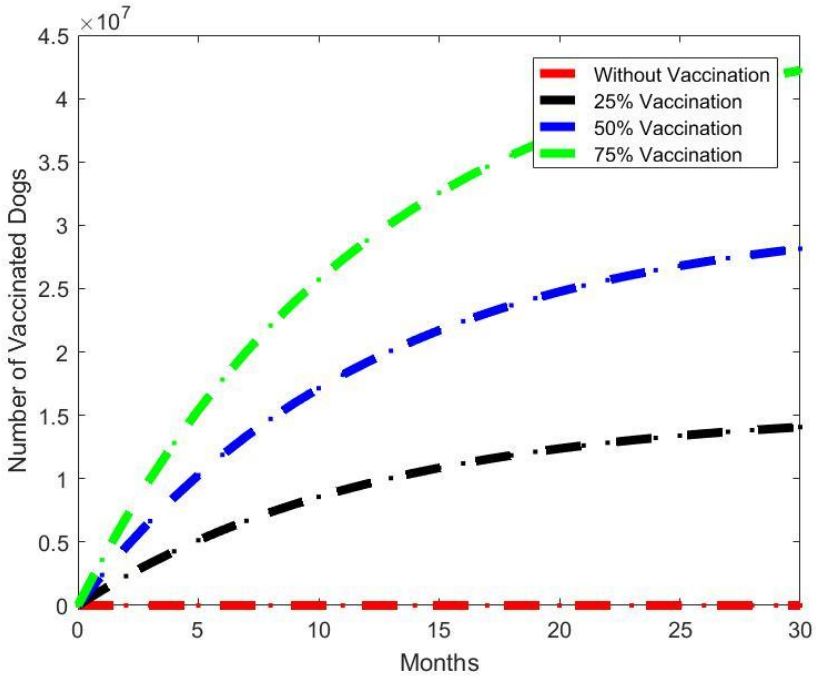

Figure 4.2: Effect of Vaccination rate on the dynamics of Vaccinated Dog Population.

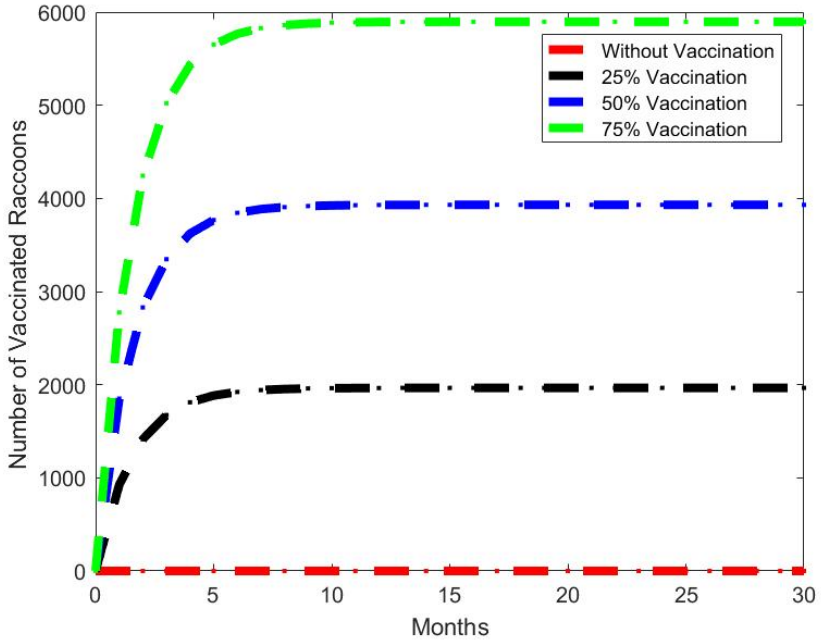

Figure 4.3: Effect of Vaccination rate on the dynamics of Vaccinated Raccoons Population.

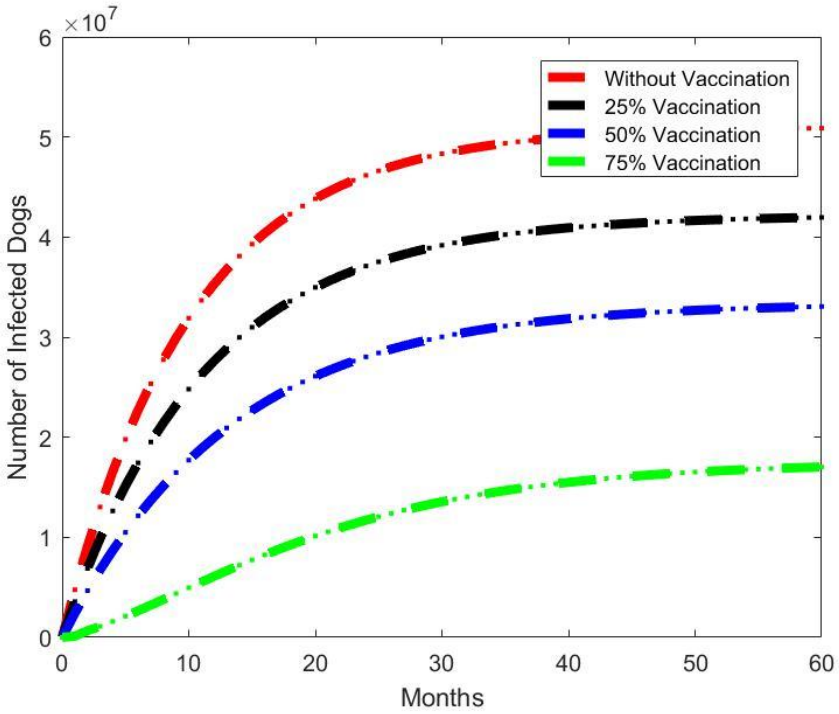

Figure 4.4: Effect of Vaccination rate on the dynamics of Infected Dogs Population.

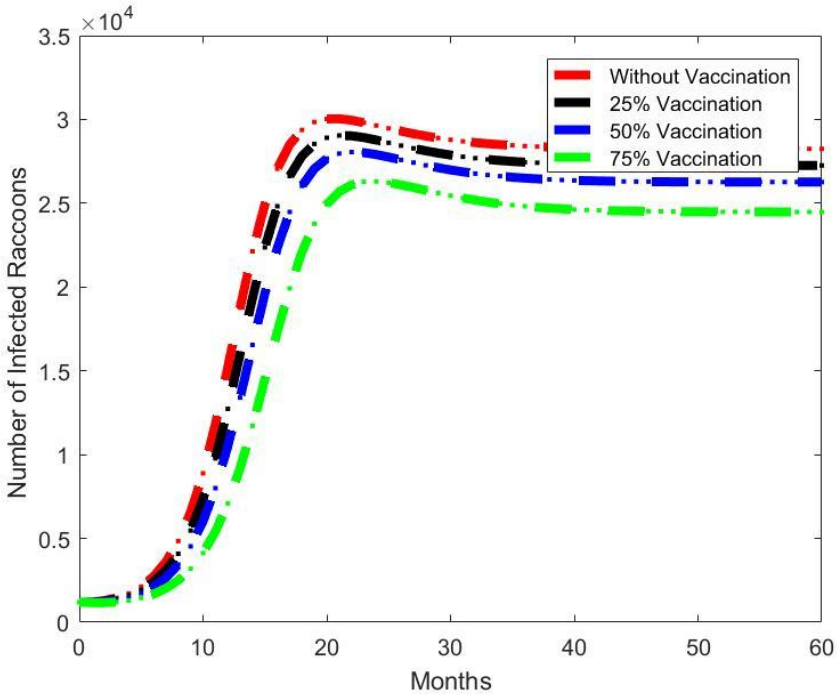

Figure 4.5: Effect of Vaccination rate on the dynamics of Infected Raccoons Population.

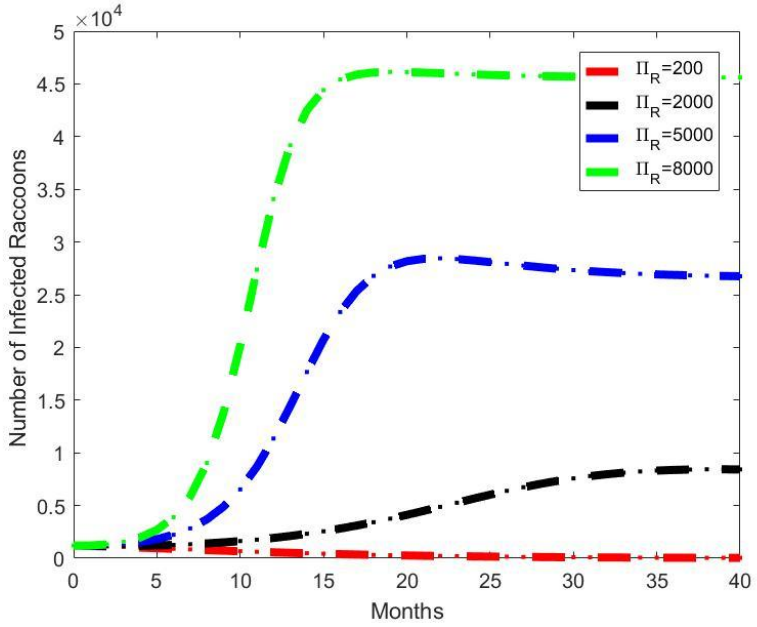

Figure 4.6: Effect of Raccoons Birth rate on the dynamics of Infected Raccoons Population.

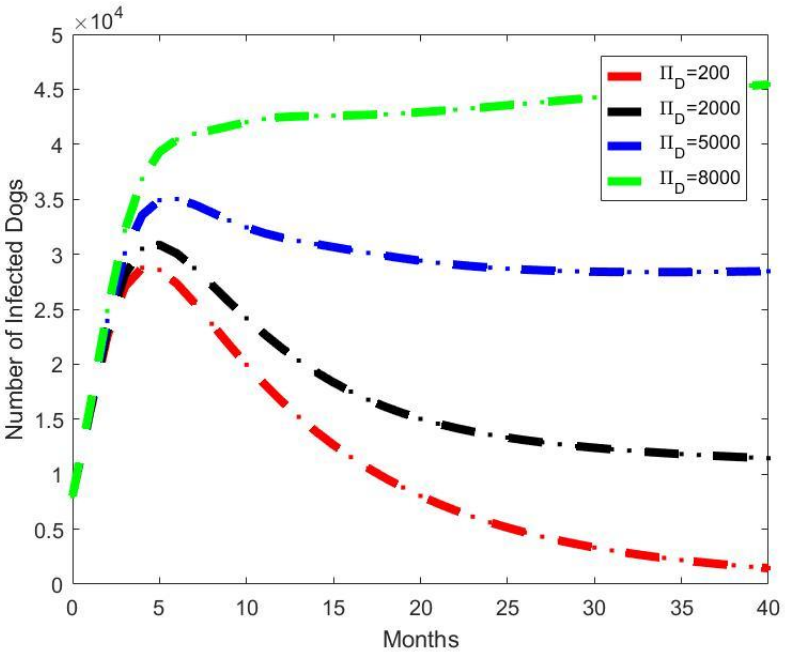

Figure 4.7: Effect of Dog Birth rate on the dynamics of Infected Dogs Population.

4.2 Discussion

The time–series plots in Figure (4.1), (4.2) and (4.3) illustrates the effect of vaccination on the vaccinated dog, human, and raccoon populations under different coverage levels (25%, 50%, and 75%), compared with the baseline scenario without vaccination. In the absence of vaccination, the vaccinated populations in all host species remain identically zero throughout the simulation period, as expected. Once vaccination is introduced, a rapid increase in the vaccinated dog population is observed during the early months, followed by a gradual leveling off toward a steady state, with higher vaccination coverage producing larger and faster accumulation of vaccinated dogs. The 75% vaccination scenario yields the highest vaccinated dog population, followed by the 50% and 25% scenarios, reflecting the progressive reduction in the pool of susceptible dogs. A similar qualitative pattern is observed in the vaccinated raccoon population, where vaccination leads to a sharp early rise and eventual saturation, with higher coverage levels resulting in substantially larger vaccinated raccoon populations. This behavior highlights the effectiveness of wildlife vaccination programs in rapidly increasing immunity within reservoir species and reducing their contribution to rabies transmission. In contrast, the vaccinated human population increases more rapidly but reaches a lower equilibrium level, reflecting the smaller size of the at-risk human population and the targeted nature of human vaccination, which is often administered as post-exposure prophylaxis. Collectively, these results demonstrate that increasing vaccination coverage across animal reservoirs significantly enhances rabies control outcomes, with dog and raccoon vaccination exerting a strong population-level impact on transmission dynamics, while human vaccination provides essential individual-level protection. These findings reinforce the established public health principle that sustained vaccination of animal reservoirs is central to rabies elimination, with human vaccination serving as a complementary intervention to prevent mortality.

The time series simulations in figures (4.4) and (4.5) clearly demonstrate that increasing vaccination coverage substantially reduces rabies prevalence in both dogs and raccoons over time. In the dog population, the absence of vaccination leads to a rapid rise in infections, stabilizing at a very high endemic level, whereas introducing vaccination progressively lowers both the growth rate and the long-term equilibrium of infected dogs, with the 75% vaccination scenario producing the most pronounced reduction and flattening of the curve. This indicates that sustained vaccination not only delays transmission but also significantly suppresses endemic persistence in dogs. A similar qualitative pattern is observed in raccoons; however, the dynamics exhibit a sharp initial outbreak followed by stabilization. Higher vaccination levels consistently reduce the peak number of infected raccoons and the eventual endemic level, although the reduction is less dramatic than in dogs, reflecting differences in transmission intensity and population turnover between the two host species. Overall, the figures highlight that vaccination is an effective control strategy in both populations, with higher coverage yielding greater epidemiological benefits, and they emphasize the critical role of mass vaccination particularly in dogs in reducing spillover risk and long-term rabies burden across interconnected host communities.

The time series results for varying both dog and raccoons birth rates in figures (4.6) and (4.7) reveals that demographic recruitment plays a critical role in shaping rabies persistence in both dogs and raccoons. As the dog birth rate increases, the number of infected dogs rises rapidly to a higher peak and settles at a substantially larger endemic level, indicating that continuous influx of susceptible dogs sustains transmission and counteracts disease-induced removal. In contrast, lower birth rates lead to a transient increase followed by a pronounced decline in infected dogs, eventually driving the system toward a much lower endemic state, which highlights the importance of population turnover in maintaining infection. The corresponding dynamics in raccoons mirror this pattern indirectly: higher dog birth rates are associated with elevated and more persistent infection levels in raccoons due to intensified cross-species transmission, whereas reduced dog recruitment diminishes spillover and lowers raccoon infection levels over time. Collectively, these figures demonstrate that controlling dog population growth through measures such as sterilization or regulated breeding can significantly reduce rabies burden not only in dogs but also in wildlife reservoirs, underscoring the interconnected nature of host populations and the importance of demographic factors in rabies control strategies.

Conclusion

In this study, a deterministic mathematical model was developed and analyzed to investigate the transmission dynamics of rabies in interacting human, dog, and raccoon populations under vaccination interventions. The model was shown to be biologically well-posed, with all solutions remaining positive and bounded within a feasible region. The basic reproduction number was derived and identified as the key threshold parameter governing disease dynamics. Analytical results established that the rabies-free equilibrium is locally and globally asymptotically stable when the reproduction number is less than unity, indicating that sustained vaccination efforts can lead to complete disease elimination. Conversely, when this threshold exceeds one, an endemic equilibrium emerges, corresponding to persistent rabies transmission. Numerical simulations supported these theoretical findings and demonstrated that increasing vaccination coverage, particularly among dogs and raccoons, significantly reduces infection prevalence and suppresses endemic persistence. The simulations also revealed that high birth rates in animal populations can undermine control efforts by continuously replenishing susceptible individuals. The findings of this study reinforce the central role of mass dog vaccination in rabies control while highlighting the importance of including wildlife reservoirs and demographic management in comprehensive control strategies. From a public health perspective, the results suggest that sustained, high-coverage vaccination combined with population control measures offers a viable pathway toward rabies elimination. Future work may extend this framework by incorporating spatial heterogeneity, time delays due to incubation periods, and optimal control strategies to further inform policy and intervention planning.

Acknowledgment

Authors are grateful to the Gombe State Polytechnic, Bajoga, Rector of the Polytechnic, Directorate of Research and Development of the Institution, and Tetfund IBR Grant 2025 intervention for their financial support throughout this research**.**

Conflict of Interest

The authors declare that there was no conflict of interest.

References

[1]. Abdullahi, M., Samuel, M., Hussein, A., & Muhammad, I. S. (2024). Dynamics of rabies transmission model in human and dog populations with time delay. International Journal of Development Mathematics, 1(1).https://doi.org/10.62054/ijdm/0101.10.

[2]. Alhassan, A., Momoh, A. A., Abdullahi, S. A., & Abdullahi, M. (2024). Mathematical Model on The Dynamics of Corruption Menace with Control Strategies. *International Journal of Science for Global Sustainability*, *10*(1), 142–153. https://doi.org/10.57233/ijsgs.v10i1.604

[3]. Addo, K. M. (2012). *An SEIR mathematical model for dog rabies: Case study of Bongo District, Ghana* (Master's dissertation). Kwame Nkrumah University of Science and Technology.

[4]. Anderson, R. M., Jackson, H. C., May, R. M., & Smith, A. M. (1981). *Population dynamics of fox rabies in Europe*. *Nature, 289*, 765–771.https://doi.org/10.1038/289765a0.

[5]. Andral, L., Aubert, M., & Blancou, J. (1982). *Radio-tracking of rabid foxes*. *Comparative Immunology, Microbiology and Infectious Diseases, 5*, 285–291.

[6]. Asano, E., Gross, L., Lenhart, S., & Real, L. A. (2008). *Optimal control of vaccine distribution in a rabies metapopulation model*. *Mathematical Biosciences and Engineering, 5*, 219–238.

[7]. Belcher, D., Wurapa, F., & Atuora, D. (1976). *Endemic rabies in Ghana: Epidemiology and control measures*.

[8]. Clayton, T., Duke-Sylvester, S., Gross, L. J., Lenhart, S., & Real, L. A. (2010). *Optimal control of a rabies epidemic model with a birth pulse*. *Journal of Biological Dynamics, 4*(1), 43–58. https://doi.org/10.1080/17513750902935216.

[9]. De la Sen, M., Ibeas, A., & Alonso-Quesada, S. (2012). *On vaccination controls for the SEIR epidemic model*. *Communications in Nonlinear Science and Numerical Simulation, 17*, 2637–2658. https://doi.org/10.1016/j.cnsns.2011.10.012.

[10]. Ega, T. T., Luboobi, L. S., & Kuznetsov, D. (2015). *Modeling the dynamics of rabies transmission with vaccination and stability analysis*. *Applied and Computational Mathematics, 4*(6), 409–419. https://doi.org/10.11648/j.acm.20150406.13.

[11]. Hethcote, H. W. (2008). *The basic epidemiology models: Models, expressions for R_0, parameter estimation, and applications*. In S. Ma & Y. Xia (Eds.), *Mathematical understanding of infectious disease dynamics* (pp. 1–61). World Scientific. https://doi.org/10.1142/9789812834836_0001.

[12]. Hou, Q., Jin, Z., & Ruan, S. (2012). *Dynamics of rabies epidemics and the impact of control efforts in Guangdong Province, China*. *Journal of Theoretical Biology, 300*, 39–47. https://doi.org/10.1016/j.jtbi.2012.01.015.

[13]. Isiyaku, M., Abdullahi, M., Husseini, A., Song, I. M., Bade, S. H., Abubakar, A., & Gidado, U. (2025). Mathematical Modeling and Analysis of Rabies Transmission Dynamics with Vaccination. *FUDMA JOURNAL OF SCIENCES*, *9*(9), 317-326. https://doi.org/10.33003/fjs-2025-0909-3733.

[14]. John, T. J., & Samuel, R. (2000). *Herd immunity and herd effect: New insights and definitions*. *European Journal of Epidemiology, 16*(7), 601–606. https://doi.org/10.1023/A:1007626510002.

[15]. Johnson, S. (2007). *Rabies*. *Ghana Veterinary Medical Association Newsletter, 6*, 18–19.

[16]. Macdonald, D. W. (1980). *Rabies and wildlife: A biologist's perspective*. Oxford University Press.

[17]. Macdonald, D. W., Bunce, R. G. H., & Bacon, P. J. (1981). *Fox populations, habitat characterization and rabies control*. *Journal of Biogeography, 8*, 145–151.

[18]. Murray, J. D., Stanley, E. A., & Brown, D. L. (1986). *On the spatial spread of rabies among foxes*. *Proceedings of the Royal Society of London. Series B, Biological Sciences, 229*(1255), 111–150. https://doi.org/10.1098/rspb.1986.0078.

[19]. Panjeti, V. G., & Real, L. A. (2011). *Mathematical models for rabies*. In A. C. Jackson (Ed.), *Advances in Virus Research* (Vol. 79, pp. 377–395). Elsevier. https://doi.org/10.1016/B978-0-12-387040-7.00018-4

[20]. Robert, H., & Williams, J. D. (1996). *Veterinary medicine: An illustrated history*. Mosby.

[21]. Russell, C. A., Smith, D. L., Childs, J. E., & Real, L. A. (2005). *Predictive spatial dynamics and strategic planning for raccoon rabies emergence in Ohio*. *PLoS Biology, 3*(3), e88. https://doi.org/10.1371/journal.pbio.0030088.

[22]. Smith, D. L., Lucey, B., Waller, L. A., Childs, J. E., & Real, L. A. (2002). *Predicting the spatial dynamics of rabies epidemics on heterogeneous landscapes*. *Proceedings of the National Academy of Sciences of the United States of America, 99*, 3668–3672. https://doi.org/10.1073/pnas.052427299.

[23]. Voigt, D. R., Tinline, R. R., & Broekhoven, L. H. (1985). *A spatial simulation model for rabies control*. In P. J. Bacon (Ed.), *Population dynamics of rabies in wildlife* (pp. 311–349). Academic Press.

[24]. Yousaf, M. Z., Qasim, M., Zia, S., Khan, M. U. R., Ashfaq, U. A., & Khan, S. (2012). *Rabies molecular virology, diagnosis, prevention and treatment*. *Virology Journal, 9*, 50. https://doi.org/10.1186/1743-422X-9-50.

[25]. Yousaf, M. Z., Qasim, M., Zia, S., Khan, M. U. R., Ashfaq, U. A., & Khan, S. (2012). *Rabies molecular virology, diagnosis, prevention and treatment*. *Virology Journal, 9*, Article 50. https://doi.org/10.1186/1743-422X-9-50.

[26]. Zhang, J., Jin, Z., Sun, G.-Q., Zhou, T., & Ruan, S. (2011). *Analysis of rabies in China: Transmission dynamics and control*. *PLoS ONE, 6*(7), e20891. https://doi.org/10.1371/journal.pone.0020891.